RSC Advances

PAPER

View Article Online
View Journal | View Issue

Cite this: *RSC Adv.*, 2026, **16**, 21438

New isohemigossypol related conjugates and caffeoylated oleanane triterpenoids from *Hibiscus syriacus* roots with anti-senescence modulating activity

Hyo-Moon Cho, †[a] Minh-Thi-Tuyet Le,†[a] Ji-Hye Shin,[a] Van-Hieu Mai,[a] Seri Choi,[a] Jin-Pyo An,[a] Yun-Sil Lee[bc] and Won-Keun Oh *[a]

Received 22nd February 2026
Accepted 9th April 2026

DOI: 10.1039/d6ra01557c

rsc.li/rsc-advances

Phytochemical investigation of the dried roots of *Hibiscus syriacus* L. led to the isolation of six previously undescribed compounds, including three rare benzo[1,4]dioxane-fused isohemigossypol conjugates (**1–3**) and three caffeoylated oleanane-type triterpenoids (**4–6**), together with 11 known compounds (**7–20**). Comprehensive spectroscopic analyses, combined with electronic circular dichroism (ECD) calculations, enabled the full structural elucidation of these metabolites and revealed isohemigossypol-derived phenylpropanoid conjugates and caffeoylated oleanane-type triterpenoids. Notably, Cell based screening identified selected compounds that suppressed $p16^{INK4A}$ (p16) promoter activity, and follow up assays in senescent fibroblasts showed reduced senescence associated readouts, including SASP related cytokine transcripts. These findings highlight *H. syriacus* as a good source of structural diversity and pharmacological potential for the discovery of previously undescribed anti aging scaffolds.

Introduction

The *Hibiscus* genus (Malvaceae), comprising over 300 species of flowering plants, is widely distributed across tropical and subtropical regions.[1] Species within this genus are globally valued for their applications in traditional medicine, ornamental horticulture, and functional foods.[2] Among them, *Hibiscus sabdariffa* L. is particularly well known and widely consumed as a herbal tea (roselle), offering antioxidant and cardioprotective benefits largely attributed to its anthocyanins and organic acid contents.[3] While *H. sabdariffa* has been the subject of extensive phytochemical research, other *Hibiscus* species have received comparatively less attention, particularly with respect to structurally diverse and nonpolar secondary metabolites. *Hibiscus syriacus* L., a deciduous shrub native to East Asia, has traditionally been used to reduce fever, promote detoxification, and enhance general wellness.[4] To date, only a limited number of secondary metabolites, including naphthalene derivatives, lignans, coumarin-lignans, and oxygenated triterpenoids, have been reported from this species, some of which exhibit significant antioxidant, anti-inflammatory, and cytotoxic activities.[5–9] Despite these findings, the full chemical diversity of *H. syriacus* remains insufficiently explored, indicating that additional structurally new and biologically relevant constituents may yet be discovered.

Hemigossypol, a prenylated naphthalene derivative belonging to the cadalene type sesquiterpenoids, first identified in *Gossypium barbadense* L. (Malvaceae), serves as a key biosynthetic precursor of gossypol.[10] Although originally thought to be specific to cotton plants, hemigossypol and its methylated analogues have since been identified in other members of the Malvaceae family, including *Kydia calycina* Roxb. and *Bombax malabaricum* DC., suggesting that the biosynthetic capacity to generate isohemigossypol-type scaffolds is more broadly conserved within the family.[11,12] This hypothesis was further supported by the isolation of isohemigossypol 1-methyl ether from *Hibiscus tiliaceus* L., providing the first chemical evidence for such metabolites within the genus.[13] Although isohemigossypol-type compounds have not been consistently detected in *H. sabdariffa*, the occurrence of structurally related prenylated naphthalene derivatives and quinones such as hibiscones and hibiscoquinones, supports the hypothesis that *Hibiscus* species possess the enzymatic machinery required to generate isohemigossypol-like frameworks.[14,15] These observations raise the possibility that underexplored species such as *H. syriacus* may harbor novel isohemigossypol-related metabolites with unique structural features and bioactivities.

[a]*Research Institute of Pharmaceutical Sciences, College of Pharmacy, Seoul National University, Seoul 08826, Republic of Korea. E-mail: wkoh1@snu.ac.k*

[b]*Graduate School of Pharmaceutical Sciences and College of Pharmacy, Ewha Womans University, Seoul 03760, Republic of Korea*

[c]*Innovative BioPharmChem Convergence Education and Research Program, Ewha Womans University, Seoul 03760, Republic of Korea*

† These authors contributed equally to this work.

Aging is a multifactorial and progressive biological process characterized by an irreversible decline across organ systems and an increased susceptibility to chronic diseases, including neurodegenerative, cardiovascular, and fibrotic diseases such as idiopathic pulmonary fibrosis (IPF).[16] A key hallmark of aging is cellular senescence, a state of stable cell-cycle arrest triggered by DNA damage, oxidative stress, oncogene activation, or telomere shortening.[17] Although senescent cells cease proliferation, they remain metabolically active and secrete pro-inflammatory mediators, cytokines, chemokines, and proteases, collectively known as the senescence-associated secretory phenotype (SASP).[18] While transient senescence aids tumor suppression and tissue repair, its chronic accumulation drives inflammation and contributes to age-related pathologies.[19] Consequently, targeting senescent cells has become a promising strategy for treating age-associated disorders. Two main pharmacological approaches are under active investigation: senolytics, which selectively eliminate senescent cells, and senomorphics, which suppress SASP or restore normal cellular function without inducing cell death.[20] Among established senescence markers, cyclin-dependent kinase inhibitor 2A (*CDKN2A*, $p16^{INK4A}$; hereafter p16) is a pivotal regulator that inhibits CDK4/6 and arrests the cell cycle at G1. However, its persistent overexpression promotes the buildup of senescent cells and chronic inflammation, linking p16 not only to cellular aging but also to tissue degeneration and impaired regeneration.[21]

In this study, as part of our ongoing efforts to identify compounds that inhibit p16 and suppress the SASPs, we report the isolation and structural characterization of three new benzo[1,4]dioxane–fused isohemigossypol conjugates (**1–3**) and three new caffeoylated oleanane-type triterpenoids (**4–6**), along with 11 known compounds (**7–20**), from the dried roots of *H. syriacus* in Fig. 1.

Results and discussion

Compound **1** was obtained as a pale yellowish amorphous powder and assigned the molecular formula $C_{23}H_{22}O_7$, as established by positive-ion HRESIMS at *m*/*z* 411.1447 $[M + H]^+$ (calcd for $C_{23}H_{23}O_7$, 411.1444). The ^1H and ^{13}C NMR spectra of **1** exhibited two ortho-coupled aromatic protons [δ_H 6.96 (1H, d, J = 8.9 Hz; δ_C 117.3) and 7.78 (1H, d, J = 8.9 Hz; δ_C 138.6)], a singlet aromatic proton [δ_H 7.20 (1H, s; δ_C 123.4)], seven aromatic nonprotonated carbons (δ_C 113.1, 166.5, 123.8, 125.4, 143.2, 137.9, and 122.1), an aldehyde group [δ_H 11.26 (1H, s; δ_C 199.1)], and a methyl group [δ_H 2.34 (3H, s; δ_C 16.1)] as the characteristic signals of the isohemigossypol skeleton.[1] In addition, a singlet aromatic proton [δ_H 6.64 (2H, s; δ_C 104.3)], two methoxyl groups [δ_H 3.93 (6H, s; δ_C 56.6)], aromatic carbons (δ_C 127.9, 104.3, 147.4, and 135.5), two mutually coupled oxymethine protons [δ_H 4.73 (1H, d, J = 8.0 Hz; δ_C 81.2) and 4.15 (1H, m; δ_C 74.5)], and a methyl group [δ_H 1.33 (3H, d, J = 6.2 Hz; δ_C 17.4)] indicated the presence of a sinapyl moiety (Fig. 1).

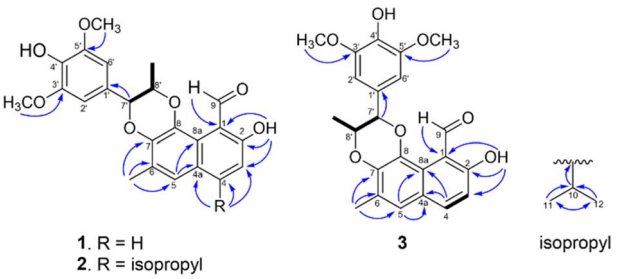

Fig. 2 Selected HMBC (arrows) and COSY (bold lines) correlations of compounds **1–3**.

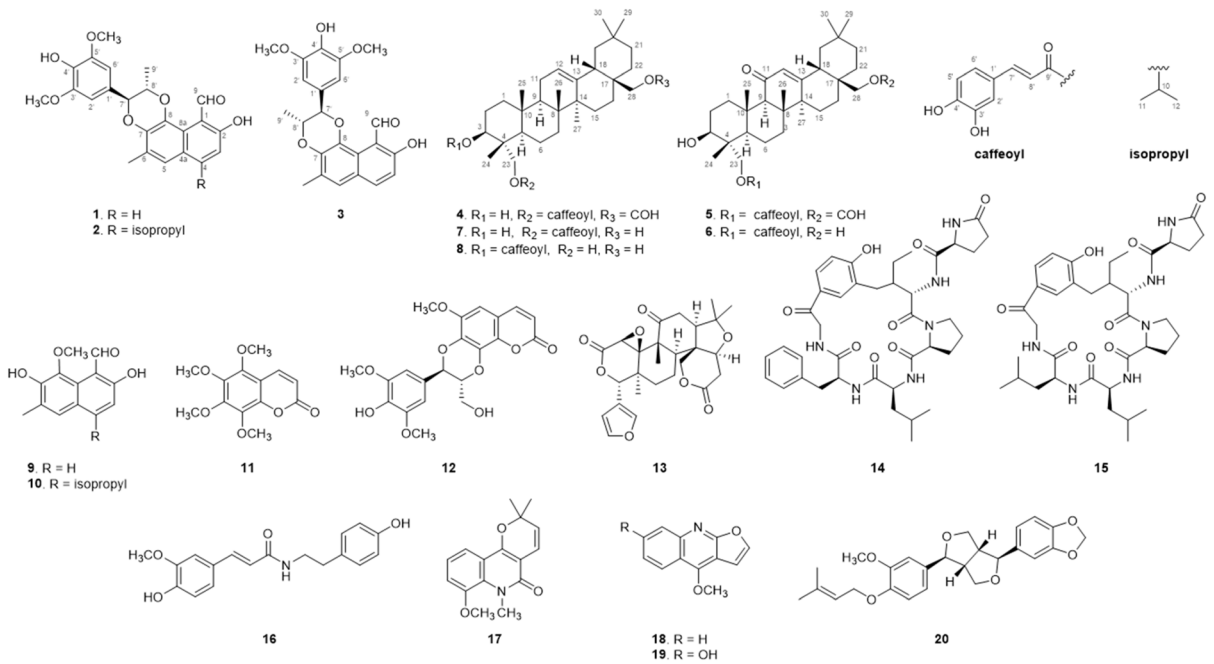

Fig. 1 Chemical structures of compounds **1–20** isolated from *H. syriacus*.

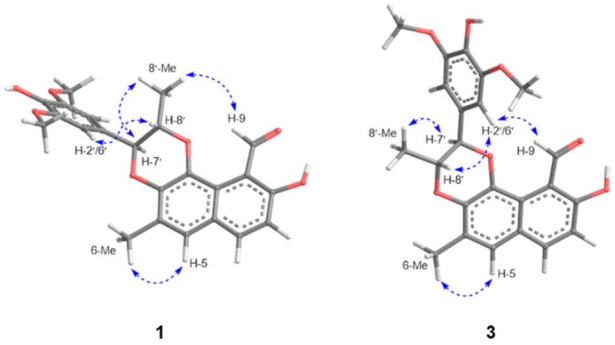

Fig. 3 Key NOESY correlations (dash arrows) of compounds **1** and **3**.

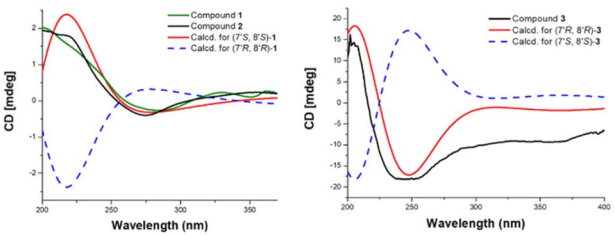

Fig. 4 Experimental and calculated ECD spectra of compounds **1** and **3**.

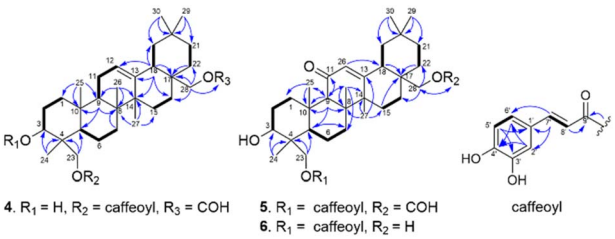

Fig. 5 Selected HMBC (arrows) and COSY (bold lines) correlations of compounds **4**–**6**.

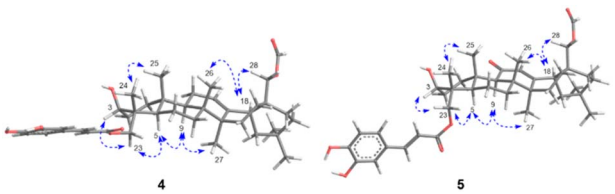

Fig. 6 Key NOESY correlations (dash arrows) of compounds **4** and **5**.

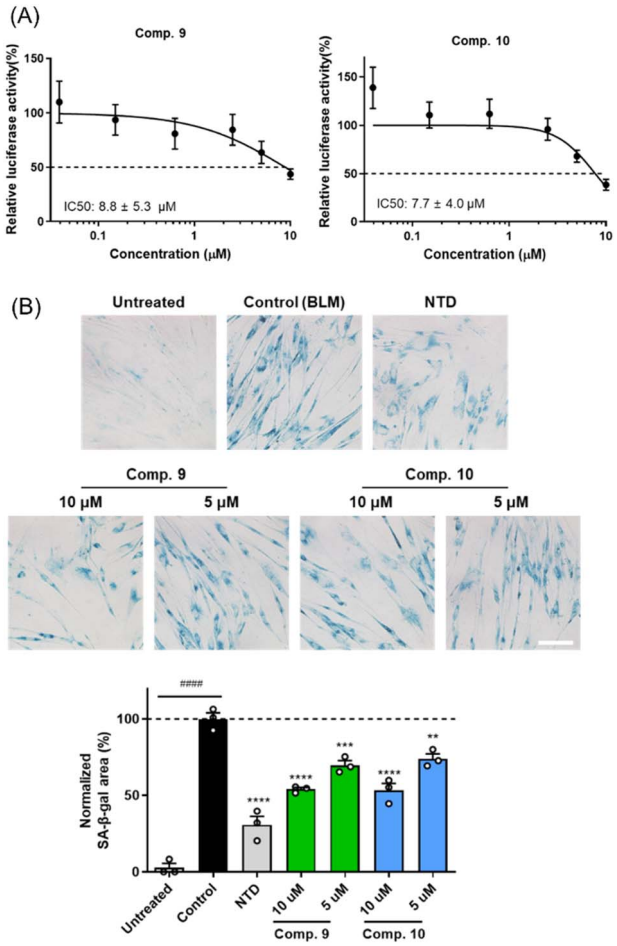

Fig. 7 Dose-dependent inhibition of p16 promoter activity and senescence-modulating effects of compounds **9** and **10**. (A) Dose-dependent inhibitory effects of compounds **9** and **10** (0.039–10 μM) on p16 promoter activity. After transfection, cells were treated with each compound for 20 h. Luciferase activity was normalized to β-galactosidase and expressed as relative values (%) compared with the untreated group. Data are presented the mean ± SEM (n = 3). (B) Senescence-associated β-galactosidase (SA-β-gal) staining of IMR-90 cells pretreated with BLM (bleomycin, 40 μg mL^{-1}) and subsequently treated with compounds **9**, **10**, or NTD (nintedanib, 5 μM; positive control) for 2 days. Data are shown as the mean ± SEM (n = 3). Values were normalized to untreated (0%) and BLM-treated (100%) conditions. Statistical significance was determined using one-way ANOVA followed by Dunn's multiple comparisons test ($^{\#\#\#\#}p$ < 0.0001 *vs.* untreated; $^{**}p$ < 0.01, $^{***}p$ < 0.001 and $^{****}p$ < 0.0001 *vs.* BLM-treated control group). Scale bar = 100 μm.

The linkage between the isohemigossypol and the phenylpropanoid moieties was elucidated by key HMBC correlations from H-7′ (δ_H 4.73) to C-1′ (δ_C 127.9) and C-8′ (δ_C 74.5), from H-8′ (δ_H 4.15) to C-7′ (δ_C 81.2) and 8′-Me (δ_C 17.4), and from 8′-Me (δ_H 1.33) to C-8 (δ_C 137.9), consistent with a 1,4-dioxane ring system, as observed in cleomiscosin C (Fig. 2).[22] Since a hemigossypol–phenylpropanoid conjugate has not been previously reported, compound **1** was initially considered to have three possible structural isomers depending on the position of the 1,4-dioxane ring. However, the structure in which the ring is formed at C-6 and C-7 was excluded because the observed HMBC correlations between 6-Me (δ_H 2.34) and H-5 (δ_H 7.20) contradicted this possibility. To further clarify the ring position, two geometrically optimized candidate structures (**1a** and **1b**) were generated and compared with NOESY data (Fig. 3 and S7, SI). The observed NOESY correlation between 8′-Me (δ_H 1.33) and H-9 (δ_H 11.26) supported the formation of a 1,4-dioxane ring connecting C-7 and C-8 within the isohemigossypol moiety. This assignment was further corroborated by the short interproton distance (3.6

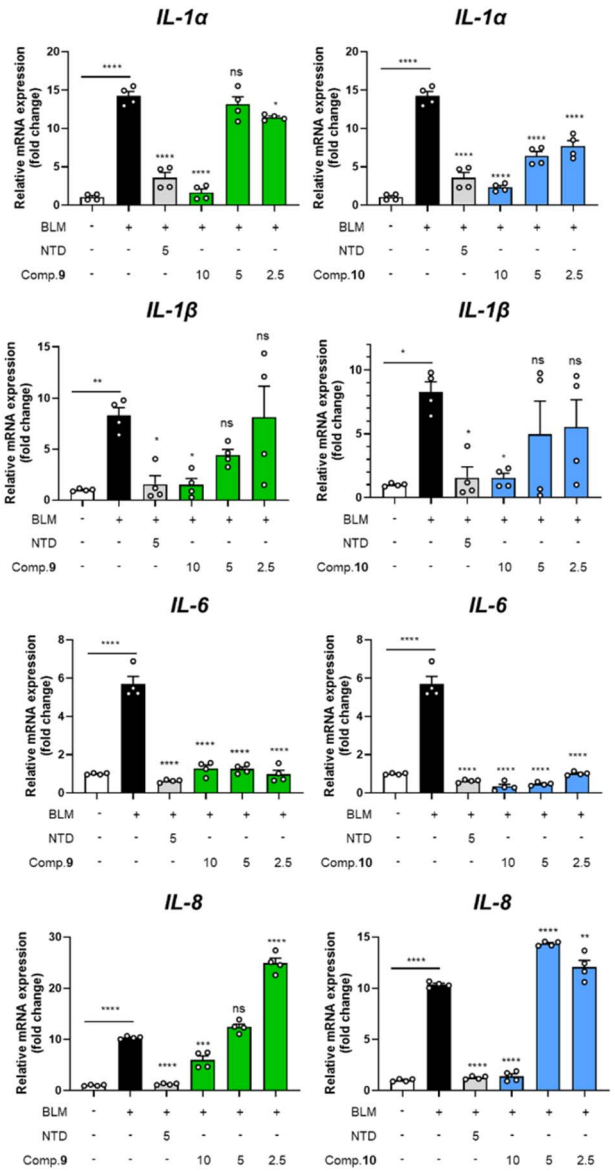

Fig. 8 Effects of compounds **9** and **10** on SASP mRNA expression in BLM-induced senescent IMR-90 cells. IMR-90 cells were exposed to BLM (bleomycin, 40 μg mL^{-1}) for 2 days and then treated with the indicated compounds including NTD (nintedanib, 5 μM; positive control), for an additional 2 days. Compounds **9** and **10** were tested in a dose-dependent manner (2.5, 5, and 10 μM) for their effects on IL-1α (A), IL-1β (B), IL-6 (C), and IL-8 (D) expression. Both compounds significantly reduced SASP gene expression compared with the BLM-treated group. Data are present as the mean ± SEM ($n = 4$). *$p < 0.05$, **$p < 0.01$, ***$p < 0.001$ *vs.* BLM-treated control; $^{\#}p < 0.05$, $^{\#\#}p < 0.01$, $^{\#\#\#}p < 0.001$ *vs.* untreated.

Å) observed in the optimized 3D model of structure **1a**. In contrast, the alternative structure (**1b**), featuring the 1,4-dioxane ring formed at C-5 and C-6, was considered unlikely because the long interproton distance (7.0 Å) between 8′-Me and H-9 was inconsistent with the observed NOESY correlations (Fig. S7, SI). The relative configuration of **1** was established as *trans*-diaxial orientation within the benzodioxane moiety, based on the NOESY correlations of H-7′ with 8′-Me and H-8′ with H-2′/6′, together with a large coupling constant ($^{3}J_{\text{H-7′/8′}} = 8.0$ Hz).[22] The absolute configuration at C-7′ and C-8′ was determined by comparison of the experimental and calculated ECD spectra. Conformational searches for two possible enantiomers [(7*S*,8*S*)-**1** and (7*R*,8*R*)-**1**] were conducted using the MMFF94s force field in CONFLEX software. ECD calculations for all generated conformers were performed at the B3LYP/6–31G level for all atoms (Fig. S52 and Table S3, SI). The experimental ECD spectrum of **1** displayed a strong positive Cotton effect (CE) at 218 nm and a weak negative CE at 279 nm, matching well with the calculated spectrum of (7′*S*,8′*S*)-**1** (Fig. 4). Accordingly, compound **1** was identified as a previously undescribed isohemigossypol–phenylpropanoid conjugate and named syriacussnu A (**1**).

Compound **2** was obtained as a pale yellowish amorphous powder and assigned the molecular formula $C_{26}H_{28}O_7$, based on positive-ion HRESIMS at *m*/*z* 453.1915 $[M + H]^+$ (calcd for $C_{26}H_{29}O_7$, 453.1913). Comparison of NMR data for compound **2** with those of **1** revealed the same isohemigossypol core fused to a phenylpropanoid moiety. However, the NMR spectra of **2** additionally showed signals corresponding to an isopropyl unit, including two methyl groups [δ_H 1.37 (6H, d, $J = 6.8$ Hz; δ_C 23.3)] and a methine group [δ_H 3.66 (1H, m; δ_C 29.5)]. The position of the isopropyl unit was deduced from HMBC cross-peaks of H-10 (δ_H 3.66) to C-3, C-4, and C-4a. The 1,4-dioxane ring in compound **2** was confirmed to occupy the same position as in **1** (attached at C-7 and C-8), as evidenced by the key NOESY correlations of H-9 (δ_H 11.20)/8′-Me (δ_H 1.33), 6-Me (δ_H 2.38)/H-5 (δ_H 7.53), and 6-Me/H-2′ and 6′ (δ_H 6.64) (Fig. S16, SI). The relative configuration of **2** was determined as *trans*-diaxial orientation between the H-7′ and H-8′, supported by the large coupling constant ($^{3}J_{\text{H-7′/8′}} = 7.9$ Hz) and NOESY correlations of H-7′ (δ_H 4.75) with 8′-Me, and H-8′ (δ_H 4.14) with H-2′/6′. Furthermore, the ECD spectrum of **2** exhibited a strong positive CE at 218 nm and a weak negative CE at 275 nm, nearly identical to that of compound **1** (Fig. 4), confirming that **2** possesses the same absolute configuration as **1**. On the basis of these data, compound **2** was identified as an isohemigossypol conjugate and was given the name syriacussnu B (**2**).

Compound **3** was obtained as a pale yellowish amorphous powder with a molecular formula $C_{23}H_{22}O_7$, as established by positive-ion HRESIMS at *m*/*z* 411.1454 $[M + H]^+$ (calcd for $C_{23}H_{23}O_7$, 411.1444). Its molecular weight was identical to that of compound **1**. Comparative NMR analysis revealed that compound **3** possesses an isohemigossypol–phenylpropanoid core similar to that of compound **1**. However, the proton chemical shifts of the two oxymethine protons [δ_H 4.64 (1H, d, $J = 7.9$ Hz; δ_C 81.3) and 4.25 (1H, m; δ_C 74.3)] in the dioxane ring showed slightly shifts, and the altered NOESY correlations in the sinapyl moiety indicated that the structure of **3** differed from that of **1** (Fig. 3). The NOESY correlations between 6-Me and the aromatic protons (H-2′/6′) of the sinapyl moiety, and between 8′-Me and H-9, which were observed in compound **1**, were absent in **3**. Instead, a new NOESY correlation between H-9 (δ_H 11.15) and H-2′/6′ (δ_H 6.62) was detected (Fig. S25, SI). These data indicated that the sinapyl unit in **3** is attached in the opposite orientation relative to that in compound **1**. The key

NOESY correlations of H-7′ (δ_H 4.64)/8′-Me (δ_H 1.29) and H-8′ (δ_H 4.25)/H-2′ and 6′ (δ_H 6.62), together with a large coupling constant ($^3J_{H\text{-}7'/8'}$ = 7.9 Hz), confirmed a *trans*-diaxial orientation of the 1,4-dioxane ring. To determine the absolute configuration of compound **3**, ECD calculations for (7′*R*,8′*R*)-**3** and (7′*S*,8′*S*)-**3** were performed using time-dependent density functional theory (TDDFT) at the B3LYP/6-31G level. The experimental ECD spectrum of compound **3**, which showed a strong positive CE at 208 nm and a strong negative CE at 250 nm, was in good agreement with the calculated spectrum of (7′*R*,8′*R*)-**3** (Fig. 4). Accordingly, compound **3** was identified as a sesquiterpene–phenylpropanoid conjugate and was given the trivial name syriacussnu C (**3**).

Compound **4** was obtained as a pale yellowish amorphous powder and found to have the molecular formula $C_{40}H_{56}O_7$, as established by negative-ion HRESIMS at *m*/*z* 647.3966 $[M - H]^-$ (calcd for $C_{40}H_{55}O_7$, 647.3948). Analysis of ^1H and ^{13}C NMR spectra revealed the presence of six tertiary methyl groups [δ_H 0.79 (3H, s; δ_C 12.8), 1.02 (3H, s; δ_C 16.4), 0.98 (3H, s; δ_C 17.3), 1.14 (3H, s; δ_C 26.5), 0.89 (3H, s; δ_C 33.6), and 0.90 (3H, s; δ_C 23.9)], an olefinic proton [δ_H 5.24 (1H, t, J = 3.7 Hz; δ_C 124.2)], a prochiral oxymethylene group [δ_H 4.03 (1H, d, J = 11.3 Hz) and 4.14 (1H, d, J = 11.3 Hz); δ_C 66.6], and a typical oxymethine proton [δ_H 3.62 (1H, dd, J = 11.8, 4.5 Hz)], attributed to a hydroxyl group at C-3 (δ_C 72.8). These spectral features are consistent with an olean-12-ene-type triterpenoid. In addition, its NMR data indicated the presence of a caffeoyl moiety, comprising a 1,3,4-trisubstituted benzene ring [δ_H 7.04 (1H, d, J = 2.0 Hz; δ_C 115.1), 6.79 (1H, d, J = 8.2 Hz; δ_C 116.5), and 6.93 (1H, dd, J = 8.2, 2.0 Hz; δ_C 123.0)], a *trans*-olefin [δ_H 7.56 (1H, d, J = 15.8 Hz; δ_C 146.9) and 6.27 (1H, d, J = 15.8 Hz; δ_C 115.1)] conjugated with a carbonyl carbon (δ_C 169.1), and an additional formyl ester group [δ_H 8.11 (1H, s; δ_C 163.1)]. The position of the caffeoyl group was established by key HMBC correlations from H-23 (δ_H 4.03 and 4.14) to C-9′ (δ_C 169.1), while the correlation between H-28 (δ_H 3.77 and 4.12) and the formyl carbon (δ_C 163.1) confirmed the site of the formyl group (Fig. 5).[23] The relative configuration of **4** was inferred from coupling constant analysis and key NOESY correlations, taking biosynthetic considerations into account.[24] The α-orientation of H-3 was indicated by a large coupling constant between H-3 and H-2β (J = 11.8 Hz), consistent with a *trans*-diaxial relationship, and a smaller coupling between H-3 and H-2α (J = 4.5 Hz), consistent with an axial-equatorial arrangement. Furthermore, NOESY correlations among H-3 (δ_H 3.62) and H-23 (δ_H 4.03 and 4.14), H-23 and H-5 (δ_H 1.23), H-5 and H-9 (δ_H 1.64), and H-9 and Me-27 (δ_H 1.14) supported the α-configuration of H-3 (Fig. 6). The β-orientation of H-18 (δ_H 2.10) was deduced from the coupling constants between H-18 and H-19β (J = 4.6 Hz; axial-equatorial) and between H-18 and H-19α (J = 13.6 Hz; *trans*-diaxial). In addition, NOESY correlations among H-18, H-28 (δ_H 3.77 and 4.12), Me-26 (δ_H 0.98), Me-25 (δ_H 1.02), and Me-24 (δ_H 0.79) confirmed that these protons share the same β-orientation. Thus, the absolute configuration of compound **4** was determined as shown, and the compound was named syriacussnu D.

Compound **5** was obtained as a pale yellowish amorphous powder. Its molecular formula ($C_{40}H_{54}O_8$) was determined by negative-ion HRESIMS at *m*/*z* 661.3732 $[M - H]^-$ (calcd for $C_{40}H_{53}O_8$, 661.3740). The NMR spectra showed signals for six tertiary methyl groups (δ_C 12.7, 17.2, 19.1, 23.9, 33.2, and 23.7), an olefinic proton [δ_H 5.54 (1H, s; δ_C 129.0)], an oxymethylene group [δ_H 4.03 (1H, d, J = 11.4 Hz) and 4.15 (1H, d, J = 11.4 Hz); δ_C 66.6] at C-23, a formyl ester group [δ_H 8.12 (1H, s; δ_C 162.8)], a characteristic oxymethine at C-3 (δ_C 72.6), a caffeoyl group exhibiting an ABX system [δ_H 7.04 (1H, d, J = 2.1 Hz; δ_C 115.2), 6.79 (1H, d, J = 8.2 Hz; δ_C 116.6), and 6.95 (1H, dd, J = 8.2, 2.1 Hz; δ_C 123.0)], and a *trans*-double bond [δ_H 7.57 (1H, d, J = 15.7 Hz; δ_C 147.0) and 6.28 (1H, d, J = 15.7 Hz; δ_C 115.1)] conjugated with a carbonyl carbon (δ_C 169.0). These features indicated that compound **5** shares the same structural core as **4**. However, a detailed comparison of their NMR data revealed a key difference. Compound **5** possesses a ketone carbon (δ_C 202.2) at C-11 instead of a methylene group [δ_H 1.93 (2H, m; δ_C 24.7)] in **4**. Key HMBC correlations from H-23 (δ_H 4.03 and 4.15) to C-9′ (δ_C 169.0) established the position of the caffeoyl group, while the cross-peaks of H-9 (δ_H 2.49) with C-11 (δ_C 202.2) and of H-28 (δ_H 3.81 and 4.06) with the formyl carbon (δ_C 162.8) confirmed the locations of the ketone and formyl ester functionalities, respectively (Fig. 5). Based on these data and NOESY correlations similar to those of compound **4** (Fig. 6), compound **5** was identified as a previously undescribed olean-12-en-11-one derivative and named syriacussnu E.

Compound **6** was isolated as a pale yellowish amorphous powder and assigned the molecular formula $C_{39}H_{54}O_7$ (negative-ion HRESIMS data at *m*/*z* 633.3787 $[M - H]^-$; calcd for $C_{39}H_{53}O_7$, 633.3791). The NMR data closely resembled those of compounds **5**, indicating an olean-12-en-11-one skeleton with six methyl groups, a ketone (δ_C 202.3), and a C-3 hydroxyl (δ_C 72.5), along with a caffeoyl moiety characterized by aromatic protons [δ_H 7.04 (1H, d, J = 2.0 Hz; δ_C 115.2), 6.79 (1H, d, J = 7.9 Hz; δ_C 116.6), and 6.95 (1H, dd, J = 7.9, 2.0 Hz; δ_C 123.0)], and a *trans*-olefin [δ_H 7.57 (1H, d, J = 15.8 Hz; δ_C 147.0) and 6.29 (1H, d, J = 15.8 Hz; δ_C 115.1)]. The most distinctive structural difference from compound **5** was the absence of the formyl group at C-28 and the appearance of an oxygenated methylene signal [δ_H 3.15 (1H, d, J = 11.4 Hz) and 3.36 (1H, d, J = 11.4 Hz)] at C-28 (δ_C 69.7) in **6**. Key HMBC correlations from H-28 to C-16, C-17, and C-22 confirmed the substitution site. NOESY correlations among H-3/H-23/H-5/H-9/H-27 established α-oriented protons, whereas correlations of Me-24/Me-25/Me-26/H-18/H-28 indicated β-configuration. Accordingly, compound **6** was elucidated as an olean-12-en-11-one-type triterpenoid and designated syriacussnu F.

The isolated compounds (**1–20**) were initially screened for their ability to regulate p16 promoter-driven transcription in A549 cells using a luciferase reporter assay (Fig. S54, SI).[25] At a concentration of 10 μM, most tested compounds retained more than 90% cell viability, as confirmed by the MTT assay, indicating that their inhibitory effects on p16 expression were not attributable to nonspecific cytotoxicity. Notably, compounds **9** and **10** displayed a clear suppressive effect on p16 promoter activity. Based on these results, both compounds were selected for dose–response evaluation to quantify their inhibitory potency (Fig. 7A). A concentration-dependent inhibition

was observed, with IC_{50} values estimated at 8.8 ± 5.3 μM for compound **9** and 7.7 ± 4.0 μM for compound **10.** Given that p16 serves as both a key effector and a canonical biomarker of cellular senescence, compounds that inhibit its promoter activity are expected to attenuate the senescence phenotype. To validate this hypothesis at the cellular level, the senescence-modulating effects of compounds **9** and **10** were evaluated in bleomycin (BLM)-induced IMR-90 fibroblasts, a well-established model of DNA damage-induced senescence.[26] Nintedanib (NTD), an approved anti-fibrotic drug known to exhibit senomorphic activity through STAT3 inhibition, was used as a positive control.[27] Consistent with the p16 promoter-based findings, both compounds **9** and **10** markedly reduced the proportion of SA-β-gal-positive cells, demonstrating senescence-attenuating efficacy comparable to that of NTD (Fig. 7B). Although BLM exposure induced a modest decrease in cell viability relative to the untreated control, co-treatment with compounds **9** and **10** did not further reduce viability and even showed a slight trend toward recovery. In addition, both compounds displayed marginally lower cytotoxicity than NTD (5 μM) under the same conditions, further supporting their non-cytotoxic senomorphic profile (Fig. S55, SI). Taken together, these results indicate that compounds **9** and **10** act as non-cytotoxic modulators of cellular senescence by downregulating p16-associated pathways. To further assess their senescence-regulating potential, we examined their effects on the expression of key senescence-associated secretory phenotype (SASP) genes in bleomycin-induced IMR-90 cells.[27] Treatment with compounds **9** and **10** resulted in a dose-dependent reduction in the mRNA levels of major proinflammatory mediators, including IL-1α, IL-1β, IL-6, and IL-8 (Fig. 8). As these cytokines are central drivers of paracrine senescence and chronic inflammation, their suppression provides further evidence supporting the senomorphic activities of compounds **9** and **10**. Altogether, these findings demonstrate that both compounds not only suppress the p16-mediated senescence pathway but also alleviate SASP-associated inflammatory signaling, thereby acting as dual modulators of the senescence phenotype.

Conclusions

Our findings highlight the remarkable structural diversity of *H. syriacus*. Several isolated compounds (**1–6**, **9**, **10**, and **13**) contained carbonyl and formyl functional groups. Interestingly, compounds (**1–3**, **9**, and **10**), along with previously reported metabolites from the *Hibiscus* genus (paravifloral A, syriacusin B, and C), displayed structural features indicative of de-isopropylation.[7] This de-isopropyl transformation is exceedingly rare in nature and has been previously observed only in a few cases, such as the guaiane-type sesquiterpenes multisins D and E from *Chloranthus multistachys* C. Pei.[28] From a biosynthetic perspective, the discovery of isohemigossypol conjugates in *Hibiscus* not only expands the phytochemical diversity of this genus but also suggests the possibility of shared or convergent biosynthetic pathways within the Malvaceae.[29] Considering that isohemigossypol scaffolds have mainly been reported from the genus *Gossypium* (cotton plants), this finding implies that similar biosynthetic pathways may also operate in other members of the Malvaceae, including *Hibiscus*, thereby warranting further study.[10,15] Notably, these metabolites were consistently detected in crude extracts during LC-MS screening using a mobile phase without formic acid, suggesting that they are unlikely to be artifacts generated during the isolation process. The characteristic oxidative functionalities and de-isopropyl transformations observed among these metabolites suggest that these processes may represent key biosynthetic features of *H. syriacus*, although direct biochemical evidence remains to be established and the possibility of non-enzymatic ring formation cannot be excluded. Importantly, most of the isolated compounds exhibited senescent-suppressive activity *in vitro* by attenuating p16 expression, a well-established biomarker of cellular senescence. Among them, syriacusin A (**9**) and isohemigossypol-1-dimethyl ether (**10**) showed the most potent inhibition of p16 promoter activity and showed clear senomorphic effects, suggesting their potential as lead scaffolds for senescence-modulating agents. Collectively, these findings highlight *H. syriacus* as a biosynthetically versatile species with distinctive structural diversity and biological significance, supporting its potential as a valuable natural source of anti-aging and senescence-modulating scaffolds. Further investigations into its biosynthetic origin, structure–activity relationship, and pharmacological mechanisms will be necessary to fully understand its therapeutic potential.

Experimental

General experimental procedures

Optical rotation values were measured on a JASCO P-2000 polarimeter using methanol as solvent (JASCO, Easton, MD, USA). UV and ECD spectra were obtained in MeOH with a 1 mm quartz cell on a Chirascan-Plus CD spectrometer (Applied Photophysics, Leatherhead, UK). IR spectra were recorded using on a JASCO FT/IR-4200 spectrometer. All NMR spectra were recorded on JEOL spectrometers (400 and 600 MHz; JEOL, Tokyo, Japan) and a Bruker AVANCE spectrometer (500 MHz; Bruker, Billerica, MA, USA) spectrometers, and resulting data were processed using the Mnova software package (v.14.2.3, Mestrelab Research S.L., A Coruña, Spain). UPLC-ESI-Q-TOF-MS analyses were carried out on a Waters Xevo G2 QTOF mass spectrometer equipped with an electrospray ionization (ESI) source (Waters, Co., Manchester, UK). Open-column chromatography was performed using Sephadex LH-20 (Sigma-Aldrich, St. Louis, MO, USA). Medium-pressure liquid chromatography (MPLC) was performed on a Biotage-Isolera One apparatus (Biotage, Charlotte, NC) equipped with Reveleris C18 flash cartridges (120 g; Grace Reveleris, New Castle, DE, USA) using mixture of MeOH and H_2O as eluents. Subfractions were examined by the thin-layer chromatography on RP-18 F254S plates (Merck, Darmstadt, Germany). Final purification of compounds was achieved by semipreparative HPLC using a Gilson system (Gilson, Villiers-le-Bel, France) equipped with an Optima Pak C_{18} column (10 × 250 mm, 5 μm, RS Tech, Seoul, Korea).

Plant material

Roots of *Hibiscus syriacus* were collected in November 2020 at the Medicinal Plant Garden, College of Pharmacy, Seoul National University (Goyang-si. Gyeonggi-do, Korea; 37° 42′ 42.6″ N, 126° 48′ 59.17″ E). The plant material was authenticated by Professor Won Keun Oh from the Seoul National University, Seoul, Republic of Korea. A voucher specimen (voucher no. 2020-07) has been deposited in the Herbarium of the Medicinal Plant Garden, College of Pharmacy, Seoul National University.

Extraction and isolation

Dried roots of *H. syriacus* (5.1 kg) were extracted with EtOH (4 × 6 L, 1 day each) at room temperature under sonication. The combined extract was evaporated under reduced pressure to yield 550 g of an orange, gummy residue. The crude extract was suspended in water and successively partitioned with *n*-hexane, ethyl acetate (EtOAc), and *n*-butanol (*n*-BuOH). The EtOAc-soluble fraction (13 g) was subjected to reversed-phase MPLC using a MeOH–H_2O gradient (10 : 90 → 100 : 0, v/v) to afford 17 subfractions (E1–E17). Fraction E8 was chromatographed on a Sephadex LH-20 column chromatography using MeOH to give six subfractions (E8.1–E8.6). Subfraction E8.5 was purified by semipreparative HPLC on an RP-C18 column (CH_3CN–H_2O, 25 : 75, v/v) to yield cleomiscosin C (**12**, 10.0 mg). Subfraction E8.6 was purified by semipreparative HPLC on an RP-C18 column (CH_3CN–H_2O, 28 : 72, v/v) to afford (*E*)-*N*-feruloytyramine (**16**, 10.0 mg). From subfraction E11, limonin (**13**, 74.2 mg) was obtained as a precipitate, whereas hibispeptin A (**14**, 9.4 mg) and B (**15**, 8.1 mg) were isolated by semipreparative RP-C18 HPLC using a CH_3CN gradient (28–100%, v/v). Fraction E12 was subjected to Sephadex LH-20 column chromatography with MeOH to give eight eluates (E12.1–E12.8). Syriacusin A (**9**, 18.1 mg) and isohemigossypol-1-dimethyl ether (**10**, 15.1 mg) were purified from subfraction E12.5 by semipreparative RP-C18 HPLC (CH_3CN–H_2O, 40 : 60, v/v). Fraction E13 was separated by Sephadex LH-20 column chromatography with MeOH to yield eight subfractions (E13.1–E13.8). Subfraction E13.3 was purified by semipreparative RP-C18 HPLC (CH_3CN–H_2O, 40 : 60, v/v) to afford 8-methoxy-*N*-methylflindersine (**17**, 4.1 mg), dictamine (**18**, 4.0 mg), and confusameline (**19**, 20.0 mg). Subfraction E13.4 was isolated by semipreparative RP-C18 HPLC (CH_3CN–H_2O, 40 : 60, v/v) to obtain syriacussnu E (**5**, 1.0 mg) and F (**6**, 5.0 mg). Subfraction E13.5 was further purified by semipreparative RP-C18 HPLC (CH_3CN–H_2O, 55 : 45, v/v) to yield (+)-piperitol-4′-*O*-γ,γ-dimethylallyl ether (**20**, 16.1 mg). Subfraction E13.6 was purified by semipreparative RP-C18 HPLC (CH_3CN–H_2O, 55 : 45, v/v) to afford syriacussnu A (**1**, 3.2 mg), B (**2**, 3.3 mg), and D (**4**, 3.1 mg). Subfraction E13.7 was purified by semipreparative RP-C18 HPLC (CH_3CN–H_2O, 45 : 60, v/v) to yield syriacussnu C (**3**, 8.3 mg). Fraction E14 was chromatographed on a Sephadex LH-20 column using MeOH to afford eight subfractions (E14.1–E14.8). Subfraction E14.1 was purified by semipreparative RP-C18 HPLC (CH_3CN–H_2O, 50 : 50, v/v) to yield 6,7,8-trimethoxycoumarin (**11**, 5.0 mg). Subfraction E14.3 was purified by semipreparative RP-C18 HPLC (CH_3CN–H_2O, 55 : 45, v/v) to afford 3β,23,28-trihydroxy-12-oleanene 23-caffeate (**7**, 20.0 mg) and 3β,23,28-trihydroxy-12-oleanene 3β-caffeate (**8**, 3.3 mg).

Syriacussnu A (1). Pale yellow, amorphous powder; $[\alpha]_D^{20}$ = −21 (*c* 0.1, MeOH); UV (MeOH) λ_{max} (log ε) 208 (3.53), 231 (3.50), 284 (2.98), 360 (2.79) nm; IR ν_{max} 3392, 2922, 1620, 1516, 1430, 1339, 1114, 1010 cm^{-1}; ^1H and ^{13}C, and 2D NMR data, see Table S1; HRESIMS *m*/*z* 411.1477 $[M + H]^+$ (calcd for $C_{23}H_{23}O_7$, 411.1444, Δ = +0.7 ppm).

Syriacussnu B (2). Pale yellow, amorphous powder; $[\alpha]_D^{20}$ = −12 (*c* 0.1, MeOH); UV (MeOH) λ_{max} (log ε) 207 (3.53), 233 (3.50), 283 (2.98), 361 (2.55) nm; IR ν_{max} 3366, 2921, 1607, 1461, 1337, 1211, 1112, 1032 cm^{-1}; ^1H and ^{13}C, and 2D NMR data, see Table S1; HRESIMS *m*/*z* 453.1915 $[M + H]^+$ (calcd for $C_{26}H_{29}O_7$, 453.1913, Δ = +0.4 ppm).

Syriacussnu C (3). Pale yellow, amorphous powder; $[\alpha]_D^{20}$ = −28 (*c* 0.1, MeOH); UV (MeOH) λ_{max} (log ε) 209 (3.61), 230 (3.57), 276 (3.08), 363 (2.81) nm; IR ν_{max} 3365, 2920, 1621, 1432, 1281, 1116 cm^{-1}; ^1H and ^{13}C, and 2D NMR data, see Table S1; HRESIMS *m*/*z* 411.1454 $[M + H]^+$ (calcd for $C_{23}H_{23}O_7$, 411.1444, Δ = +2.4 ppm).

Syriacussnu D (4). Pale yellow, amorphous powder; $[\alpha]_D^{20}$ = −13 (*c* 0.1, MeOH); UV (MeOH) λ_{max} (log ε) 200 (3.89), 329 (3.68) nm; IR ν_{max} 3361, 2928, 1695, 1601, 1514, 1462, 1384, 1260, 1160, 1026 cm^{-1}; ^1H and ^{13}C, and 2D NMR data, see Table S2; HRESIMS *m*/*z* 647.3966 $[M - H]^-$ (calcd for $C_{40}H_{55}O_7$, 647.3948, Δ = +2.8 ppm).

Syriacussnu E (5). Pale yellow, amorphous powder; $[\alpha]_D^{20}$ = −14 (*c* 0.1, MeOH); UV (MeOH) λ_{max} (log ε) 200 (3.60), 247 (3.53), 330 (3.34) nm; IR ν_{max} 3392, 2944, 1602, 1455, 1385, 1261, 1165, 1032 cm^{-1}; ^1H and ^{13}C, and 2D NMR data, see Table S2; HRESIMS *m*/*z* 661.3732 $[M - H]^-$ (calcd for $C_{40}H_{53}O_8$, 661.3740 Δ = −1.2 ppm).

Syriacussnu F (6). Pale yellow, amorphous powder; $[\alpha]_D^{20}$ = −14 (*c* 0.1, MeOH); UV (MeOH) λ_{max} (log ε) 203 (3.71), 247 (3.72), 329 (3.61) nm; IR ν_{max} 3392, 2946, 1643, 1516, 1463, 1385, 1260, 1166, 1040 cm^{-1}; ^1H and ^{13}C, and 2D NMR data, see Table S2; HRESIMS *m*/*z* 633.3787 $[M - H]^-$ (calcd for $C_{39}H_{53}O_7$, 633.3791, Δ = −0.6 ppm).

Computational ECD analysis of syriacussnu A–C (1–3)

A conformational search was conducted using the CONFLEX 8 program (CONFLEX Corp., Tokyo, Japan) employing the molecular mechanics force field (MMFF94s) with an energy window of 1.0 kcal mol^{-1}. The geometry optimization of the ground-state conformers was performed at the B3LYP/def-SV(P) level in the gas phase. The optimized conformers were then subjected to time-dependent density functional theory (TDDFT) calculations at the B3LYP/6-31G level (COSMOlogic GmbH, Leverkusen, Germany). The calculated ECD spectra were obtained by Boltzmann-weighted averaging of individual conformers and visualized using SpecDis (version 1.71, Berlin, Germany).

Cell culture

The human lung cancer cell line A549 and normal lung fibroblast IMR90 (ATCC CCL-186) were obtained from the Korean

Cell Line Bank (Seoul, Republic of Korea) and the American Type Culture Collection (Manassas, VA, USA), respectively. A549 cells were maintained in RPMI-1640 medium (Welgene, Daegu, Republic of Korea), and IMR90 cells were grown in Minimum Essential Medium (MEM; Gibco, USA). Both media were supplemented with 10% fetal bovine serum (FBS; Gibco, MA, USA) and 1% penicillin-streptomycin (Hyclone, Logan, UT, USA). All cells were incubated at 37 °C in a humidified atmosphere containing 5% CO_2.

Luciferase reporter assay for p16 promoter activity

A549 cells were seeded at 8×10^3 cells per well in 96-well plates and allowed to attach for 24 h. The cells were washed with phosphate-buffered saline (PBS) and transfected for 7 h in Opti-MEM medium (Gibco, MA, USA) using Lipofectamine 2000 (Invitrogen, Carlsbad, CA, USA) and a plasmid mixture containing pGL3_p16 (0.07 μg) and pSV-β-galactosidase (0.03 μg; Promega, Madison, WI, USA) as an internal control. After transfection, the cells were treated for 20 h with the test compounds or navitoclax (positive control), lysed with cell culture lysis buffer (Promega), and assayed for firefly luciferase activity using a luciferase assay kit (Promega). Values were normalized to β-galactosidase activity.

Cell viability assay

A549 cells were seeded at 8×10^3 cells per well in 96-well plates and pre-incubated for 24 h. The cells were then treated with the indicated compounds for an additional 24 h. Cell viability was determined using the MTT [(3-(4,5-dimethyl-2-thiazolyl)-2,5-diphenyl-2H-tetrazolium bromide) assay (Sigma-Aldrich, St. Louis, MO, USA). After treatment, 20 μL of a 2 mg mL^{-1} MTT solution was added to each well, and the plates were incubated for 4 h at 37 °C in the dark. The supernatant was discarded, the formazan crystals were dissolved in 100 μL DMSO, and absorbance was measured at 540 nm using a microplate reader (VersaMaxTM, Molecular Devices, San Jose, CA, USA).

Senescence-associated β-galactosidase staining

IMR90 cells were plated at 5×10^3 cells per well in 96-well plates and cultured for 24 h. Senescence was induced by treatment with bleomycin (40 μg mL^{-1}; Tokyo Chemical Industry, Tokyo, Japan) for 48 h, except for the untreated control group, followed by exposure to the test compounds for another 48 h. SA-β-gal activity was detected using a commercial staining kit (#9860, Cell Signaling Technology, Danvers, MA, USA) according to the manufacturer's instructions. The stained cells were examined using a microscope (Olympus Corp., Tokyo, Japan). All experiments were performed in triplicate, and β-galactosidase staining intensity was quantified relative to the control group.

RNA isolation and quantitative real-time PCR analysis

IMR90 cells were seeded at 5×10^3 cells per well and cultured for 24 h. Cellular senescence was induced by bleomycin treatment (40 μg mL^{-1}; Tokyo Chemical Industry) for 48 h, except for the untreated control group, followed by exposure to the test compounds for an additional 48 h. Total RNA was extracted using NucleoZOL reagent (Macherey-Nagel, Duren, Germany), and 1 μg of RNA was reverse-transcribed into complementary DNA (cDNA) using a cDNA synthesis kit (Thermo Fisher Scientific, Waltham, MA, USA). Quantitative real-time PCR was performed using AccuPower 2 × GreenStarTM qPCR Master Mix (Bioneer, Daejon, Republic of Korea). All reactions were conducted in triplicate, and gene-expression levels were normalized to 18 s rRNA.

Statistical analysis

Data were analyzed using GraphPad Prism version 10.4.1 (GraphPad Software, Inc., La Jolla, CA, USA) and are presented as the mean ± standard error of the mean (SEM) from three independent experiments. Differences among groups were evaluated using one-way analysis of variance (ANOVA) followed by Dunn's multiple comparison post hoc test. *$p < 0.05$, **$p < 0.01$, ***$p < 0.001$, and ****$p < 0.0001$.

Author contributions

Hyo-Moon Cho: writing original draft, investigation, formal analysis, data curation. Minh-Thi-Tuyet Le: data curation, investigation, writing review and editing. Ji-Hye Shin: methodology. Van-Hieu Mai: formal analysis, data curation. Seri Choi: methodology. Jin-Pyo An: formal analysis, investigation. Yun-Sil Lee: formal analysis, data curation. Won-Keun Oh: writing – review & editing, project administration, conceptualization. All authors have read and agreed to the published version of the manuscript.

Conflicts of interest

The authors declare that they have no known competing financial interests or personal relationships that could have appeared to influence the work reported in this paper.

Data availability

The data supporting the findings of this study are included within the article and its supplementary information (SI). Supplementary information: spectroscopic data, as well as the NMR, HRESIMS, and IR spectra of new compounds **1–6**, 3D structural model of main conformers, calculated energies and coordinates of major conformers, and biological evaluation of isolated **20** compounds on p16 promoter activity and cellular senescence. Additional data related to this work are available from the corresponding author upon reasonable request. See DOI: https://doi.org/10.1039/d6ra01557c.

Acknowledgements

This research was supported by grants from the Basic Science Research Program (RS-2022-NR070150) and (RS-2023-00218616) through the National Research Foundation of Korea (NRF) funded by the Ministry of Science and ICT in Korea.

References

1 P. Dhar, C. S. Kar, D. Ojha, S. K. Pandey and J. Mitra, *Ind. Crops Prod.*, 2015, **77**, 323–332.
2 M. Kapoor, G. Kaur, N. Kaur, C. Sharma, K. Batra and D. Singh, *Eur. J. Med. Plants*, 2021, **32**, 1–37.
3 S. Najafpour Boushehri, R. Karimbeiki, S. Ghasempour, S.-S. Ghalishourani, M. Pourmasoumi, A. Hadi, M. Mbabazi, Z. K. Pour, M. Assarroudi, M. Mahmoodi, A. Khosravi, F. Mansour-Ghanaei and F. Joukar, *Phytother. Res.*, 2020, **34**, 329–339.
4 A. Balkrishna, S. Mishra, A. Singh, D. Srivastava, S. Singh and V. Arya, *J. Phytopharmacol.*, 2022, **11**, 204–210.
5 W. A. H. M. Karunarathne, I. M. N. Molagoda, S. R. Park, J. W. Kim, O.-K. Lee, H. Y. Kwon, M. Oren, Y. H. Choi, H. W. Ryu, S.-R. Oh, W. S. Jo, K. T. Lee and G.-Y. Kim, *Biomolecules*, 2019, **9**, 645.
6 S.-J. Lee, Y.-S. Yun, I.-K. Lee, I.-J. Ryoo, B.-S. Yun and I.-D. Yoo, *Planta Med.*, 2007, **65**, 658–660.
7 L.-S. Shi, C.-H. Wu, T.-C. Yang, C.-W. Yao, H.-C. Lin and W.-L. Chang, *Fitoterapia*, 2014, **97**, 184–191.
8 S. W. Yeon, H. Y. Kwon, J. I. Nam, J. H. Ahn, Y. H. Jo, A. Turk, Y. J. Lee, D. H. Shin, B. Y. Hwang and M. K. Lee, *Phytochem. Lett.*, 2019, **33**, 110–113.
9 B.-S. Yun, I.-J. Ryoo, I.-K. Lee, K.-H. Park, D.-H. Choung, K.-H. Han and I.-D. Yoo, *J. Nat. Prod.*, 1999, **62**, 764–766.
10 T. A. Wagner, J. Liu, R. D. Stipanovic, L. S. Puckhaber and A. A. Bell, *J. Agric. Food Chem.*, 2012, **60**, 2594–2598.
11 K. C. Joshi, P. Singh and S. Taneja, *Planta Med.*, 2007, **49**, 127.
12 A. V. B. Sankaram, N. S. Reddy and J. N. Shoolery, *Phytochemistry*, 1981, **20**, 1877–1881.
13 T. Matsumoto, D. Imahori, K. Achiwa, Y. Saito, T. Ohta, T. Yoshida, N. Kojima, M. Yamashita, Y. Nakayama and T. Watanabe, *Fitoterapia*, 2020, **142**, 104524.
14 S. Ali, P. Singh and R. H. Thomson, *J. Chem. Soc., Perkin Trans. 1*, 1980, 257–259.
15 A. Sotelo, H. Villavicencio, I. Montalvo and M. T. Gonzalez-Garza, *Afr. J. Tradit., Complementary Altern. Med.*, 2005, **2**, 4–12.
16 J. Guo, X. Huang, L. Dou, M. Yan, T. Shen, W. Tang and J. Li, *Signal Transduct. Target. Ther.*, 2022, **7**, 391.
17 C. López-Otín, M. A. Blasco, L. Partridge, M. Serrano and G. Kroemer, *Cell*, 2013, **153**, 1194–1217.
18 B. Wang, J. Han, J. H. Elisseeff and M. Demaria, *Nat. Rev. Mol. Cell Biol.*, 2024, **25**, 958–978.
19 W. Huang, L. J. Hickson, A. Eirin, J. L. Kirkland and L. O. Lerman, *Nat. Rev. Nephrol.*, 2022, **18**, 611–627.
20 E. U. Alum, S. C. Izah, D. E. Uti, O. P.-C. Ugwu, P. A. Betiang, M. Basajja and R. I. Ejemot-Nwadiaro, *Drug Des. Dev. Ther.*, 2025, **19**, 8489–8522.
21 J. Li and M. J. Poi, *Biochemistry*, 2011, **50**, 5566–5582.
22 B.-S. Yun, I.-K. Lee, I.-J. Ryoo and I.-D. Yoo, *J. Nat. Prod.*, 2001, **64**, 1238–1240.
23 K. W. Woo, J. Y. Han, S. U. Choi, K. H. Kim and K. R. Lee, *Nat. Prod. Sci.*, 2014, **20**, 71–75.
24 R. Thimmappa, K. Geisler, T. Louveau, P. O'Maille and A. Osbourn, *Annu. Rev. Plant Biol.*, 2014, **65**, 225–257.
25 J.-P. Coppé, F. Rodier, C. K. Patil, A. Freund, P.-Y. Desprez and J. Campisi, *J. Biol. Chem.*, 2011, **286**, 36396–36403.
26 K. Aoshiba, T. Tsuji and A. Nagai, *Eur. Respir. J.*, 2003, **22**, 436–443.
27 M. J. Schafer, T. A. White, K. Iijima, A. J. Haak, G. Ligresti, E. J. Atkinson, A. L. Oberg, J. Birch, H. Salmonowicz, Y. Zhu, D. L. Mazula, R. W. Brooks, H. Fuhrmann-Stroissnigg, T. Pirtskhalava, Y. S. Prakash, T. Tchkonia, P. D. Robbins, M. C. Aubry, J. F. Passos, J. L. Kirkland, D. J. Tschumperlin, H. Kita and N. K. LeBrasseur, *Nat. Commun.*, 2017, **8**, 14532.
28 X.-J. Wang, S.-Z. Yu, J.-L. Xin, L.-L. Pan, J. Xiong and J.-F. Hu, *Fitoterapia*, 2022, **156**, 105068.
29 H.-Y. Kwon, J.-H. Kim, S.-H. Kim, J.-M. Park and H. Lee, *Mitochondrial DNA, Part A*, 2016, **27**, 3668–3669.